

Fault analysis in rotating machines by using differential directional operators on thermal images

Hermes Alexander Fandiño Toro
Julio César García Álvarez
Germán Castellanos Domínguez

March 13, 2012

- 1 Introduction
- 2 Problem statement
- 3 Methodology
- 4 Conclusions

- 1** Introduction
- 2 Problem statement
- 3 Methodology
- 4 Conclusions

Advantages of thermal imaging for machine inspection

- Analysis of thermal images allows machine to be evaluated under different operation conditions without the need for physical contact.
- Thermal distribution alterations on some regions of image can predict the presence of a different type of failures.

- 1 Introduction
- 2 Problem statement**
- 3 Methodology
- 4 Conclusions

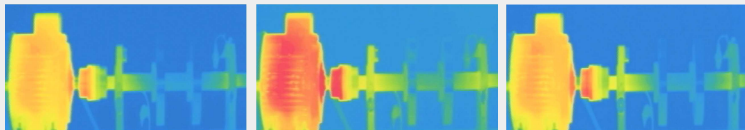
Current approaches on rotative machine inspection

- Motor operation estimation by using data and signal-based models [Bellini *et al.* 2004]. However, model-based approaches become very complex, due to the variability of the different materials being inspected.
- Fault detection by acoustic and vibration measurement and signal analysis [Tse *et al.*, 2004], [Peng *et al.*, 2005]. Nonetheless, measurement is partially-invasive and would implicate the usage of additional measurement equipment on the inspected machine.

Thermal image representation [Younus and Yang, 2010]

- Image is mapped into a multi-resolution scheme using Discrete Wavelet Transform.
- Different types of faults can be identified by value variation of some statistical measure accomplished on approximation wavelet coefficients.
- An especial kind of statistical measures –the shape measures–, are used considering that data distribution follows a unimodal probability function.
- Just one *Region of Interest* (ROI) is considered for the analyzed conditions → the localization of identified fault is not possible.

Motor operating conditions



(a) Normal operation

(b) First wheel unbalance (FWU)

(c) Second wheel unbalance (SWU)

Figure 1: Test bench image acquired at the same time point (7200s) under 3 different operating conditions.

Hypothesis

- A fault alters not only the temperature distribution but the heat propagation direction.
- Temperature alterations propagate within the boundaries of inspected parts.
- ROI can be segmented by identifying hot spots on inspected parts.

Objectives

- Fault identification by using directional operators instead statistical measures.
- An automatic ROI segmentation method leads to improve the identification of hot spots inside inspected parts.
- Fault localization can be implemented on this proposed methodology.

- 1 Introduction
- 2 Problem statement
- 3 Methodology**
- 4 Conclusions

Fault identification by differential directional operator analysis on thermal images

- Test bench,
- Thermal image preprocessing,
- Feature extraction,
- Relevance analysis,
- Performance evaluation.

Test bench

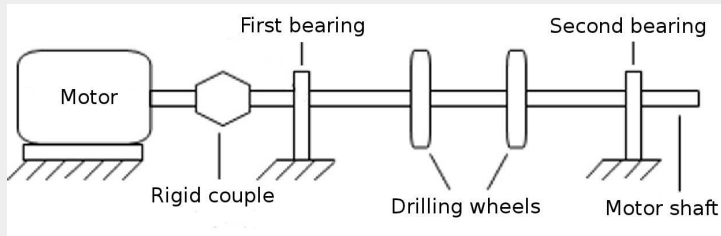


Figure 1: By attaching 5g-weighted masses inside the drilling wheels, two types of unbalance are induced, whose labels are described according to its nearest bearing.

Thermal camera set-up

(FLIR A320 camera)	Emissivity	0.82
	Reflected temperature	20°C
	Distance to test bench	1.5m
	Relative humidity	50%
	Ambient temperature	20°C
	Thermal scale	10 – 50°C
Video settings	Image size	640 × 480 pixels
	Frame rate	1 fps
	Image format	MPEG-2

Table 1: Camera settings

Image acquisition and database

- 2-hour (3600s) recordings per three operating condition types: Normal condition to **normal**, First Wheel Unbalance to **fwu** and Second Wheel Unbalance → **swu**.
- Framing by 1 frame per second.
- Acquired frames are down-sampled to one frame each 60s.
- A total of 53 images for each condition are accomplished.
- RGB and YCbCr color spaces are either considered.

Background remotion - Multilevel thresholding

- 1 Define range $\mathbf{R} = [a, b]$ where $a = \min(I)$ and $b = \max(I)$.
- 2 Define subrange limit $T_1 = \mu - k_1\sigma$ and $T_2 = \mu + k_1\sigma$, where μ and σ are calculated for R .
- 3 Pixels in intervals $[a, T_1]$ and $[T_2, b]$ are quantized to its weighted means.
- 4 For next iteration: $a = T_1 + 1$, $y b = T_2 - 1$. Do the same while difference between T_2 and T_1 is greater than 1.

A-priori ROIs

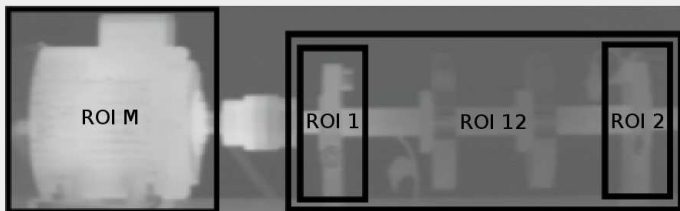


Figure 1: A-priori arbitrary-selected ROIs

Color spaces

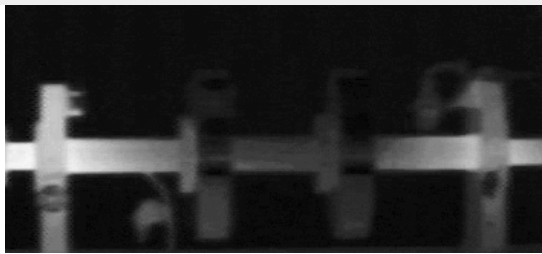


Figure 1: Infrared image - Luminance layer in YCbCr color space.

Color spaces

- Thermal images are conventionally provided by three color planes. Nonetheless, just one color plane should be used for the feature extraction process.
- In our case, a thermal gray-scale image is projected into a RGB space, providing three color planes with approximately the same thermal value (even for γ -corrected images). Therefore, any of those three planes can be used.
- However, projection of thermal values on color planes is non-linear. Therefore, a chroma-intensity transformation is more convenient for carrying information of color planes into a single plane. So, the intensity plane Y of the YC_bC_r space is suggested for usage at the feature extraction process.

Image quantization and segmentation

After multilevel thresholding is used, the image is quantized into pixel value intervals. High-valued intervals are selected to segment the image.

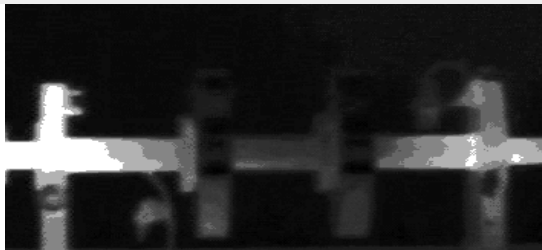


Figure 1: Quantized image.

ROI masking

After segmentation, ROI masks are carried out, whose pixel locations are saved to further analysis.



Figure 1: ROI masks (in white).

Automatically detected ROIs



Figure 1: Detected ROIs

Sobel edge detection operator

Discrete differentiation operators computing a gradient approximation of the image intensity function [Jin-Yu et al. 2009].

$$T_x = \begin{bmatrix} -1 & 0 & +1 \\ -2 & 0 & +2 \\ -1 & 0 & +1 \end{bmatrix}$$

$$T_x = \begin{bmatrix} -1 & -2 & -1 \\ 0 & 0 & 0 \\ +1 & +2 & +1 \end{bmatrix}$$

Prewitt edge detection operator

Discrete differentiation operators computing a gradient approximation of the image intensity function [Gonzalez & Woods, 2002].

$$T_x = \begin{bmatrix} -1 & 0 & +1 \\ -1 & 0 & +1 \\ -1 & 0 & +1 \end{bmatrix}$$

$$T_x = \begin{bmatrix} -1 & -1 & -1 \\ 0 & 0 & 0 \\ +1 & +1 & +1 \end{bmatrix}$$

Convolution with filtering masks

Gradient operator is implemented on a linear filter of size $m \times n$, carried out on image f of size $M \times N$ [Gonzalez & Woods, 2002]:

$$g(x, y) = \sum_{i=-a}^a \sum_{t=-b}^b w(s, t) f(x + s, y + t) \quad (1)$$

Direction angle of gradient vector

Approximation to the second derivative:

$$\alpha(x, y) = \tan^{-1} \frac{G_y}{G_x} \quad (1)$$

$$G_x = T_x * f; \quad (2)$$

$$G_y = T_y * f; \quad (3)$$

Finding of relevant angles

After convolution between image and gradient operators, a histogram of angle direction is obtained in order to search for relevant angles (features).

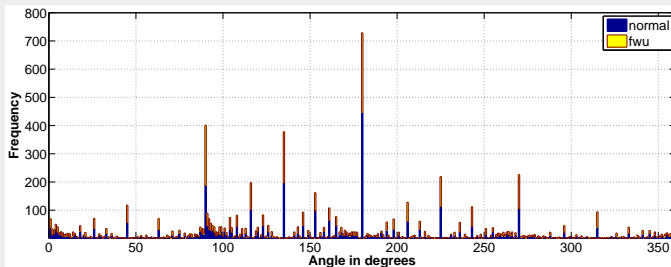


Figure 2: Stacked histogram for 2 frames of the test bench under different operation condition, at same time.

Principal Component Analysis (PCA)

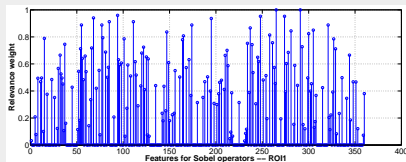
Relevant angles are found by the vector P of Q number of features:

$$P^T P = U \sqrt{(\lambda)} V^T \in Q \times Q \quad (4)$$

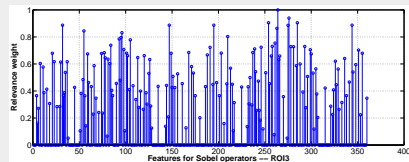
where:

- U : Eigenvalues matrix;
- λ : Eigenvector.

Results using Sobel operator



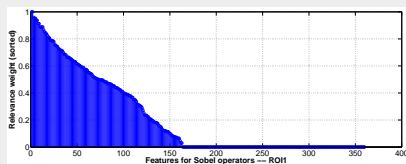
(a) RGB colorspace



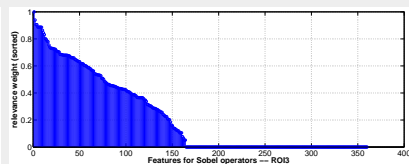
(b) YCbCR colorspace

Figure 2: Relevance analysis for features inside ROI1 and ROI3.

Results using Sobel operator



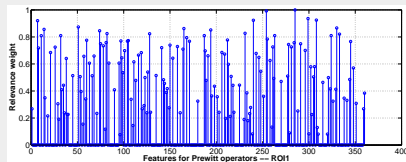
(a) RGB colorspace



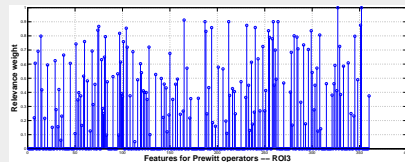
(b) YCbCR colorspace

Figure 2: Relevance analysis for features inside ROI1 and ROI3.

Results using Prewitt operator



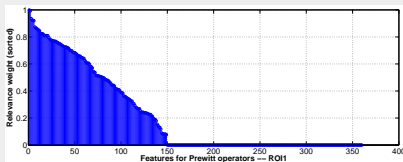
(a) RGB colorspace



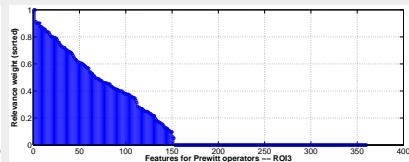
(b) YCbCR colorspace

Figure 2: Relevance analysis for features inside ROI1 and ROI3.

Results using Prewitt operator



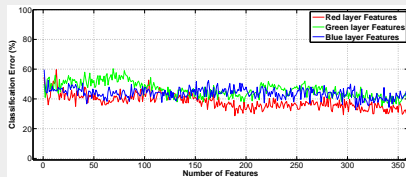
(a) RGB colorspace



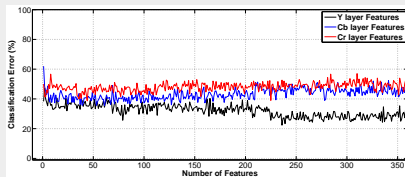
(b) YCbCR colorspace

Figure 2: Relevance analysis for features inside ROI1 and ROI3.

Classification error – Sobel operator, ROI 1



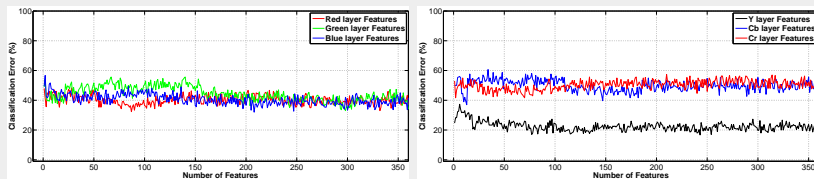
(a) RGB colorspace



(b) YCbCR colorspace

Figure 3: Classification error for ROI1 (first wheel) using Sobel operator.

Classification error – Sobel kernel, ROI 1

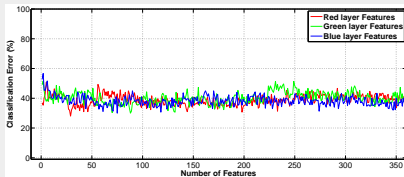


(a) RGB colorspace

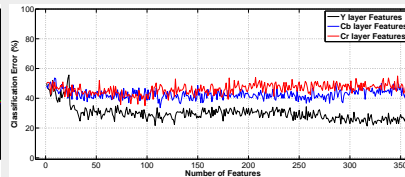
(b) YCbCr colorspace

Figure 3: Classification error for ROI3 (second wheel) using Sobel operator.

Classification error – Sobel kernel, ROI 1



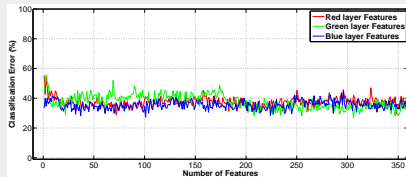
(a) RGB colorspace



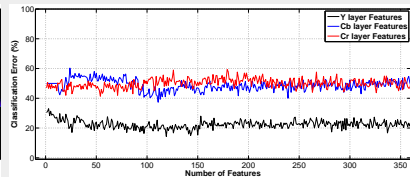
(b) YCbCR colorspace

Figure 3: Classification error for ROI1 (first wheel) using Prewitt operator.

Classification error – Sobel kernel, ROI 1



(a) RGB colorspace



(b) YCbCr colorspace

Figure 3: Classification error for ROI3 (second wheel) using Prewitt operator.

- 1 Introduction
- 2 Problem statement
- 3 Methodology
- 4 Conclusions**

Conclusions and Future Works

- The high contrast of thermal values between pixels located within hot-spots and background is the key aspect for the improvement of the proposed segmentation method.
- The relevant angles fit with the directions where the hot-spot propagation is detected, meaning an improvement for the fault interpretation. In this context, an increase of the number of relevant angles suspects that a fault occurs.
- Assuming the correspondence between relevant angles and heat propagation directions, directional patterns will be used as texture operators for a closer characterization of hot spots related with faults.

- [1] [Bellini et al, 2008] A. Bellini, F. Filippetti, C. Tassoni, and G. Capolino, "*Advances in diagnostic techniques for induction machines*," in IEEE Transactions on Industrial Electronics, vol. 55, no. 12, pp. 4109-4126, 2008.
- [2] P. Tse, W. Yang, and H. Tam, "*Machine fault diagnosis through an effective exact wavelet analysis*," in Journal of Sound and Vibration, vol. 277, no. 4-5, pp. 1005-1024, 2004.
- [3] A. Younus and B. Yang, "*Wavelet co-efficient of thermal image analysis for machine fault diagnosis*," in Proceedings of the International Conference on Mechanical Engineering, ICME09., 2009, pp. 1-6.
- [4] Z. Peng, P. Tse, and F. Chu, "*An improved hilbert-huang transform and its application in vibration signal analysis*," Journal of Sound and Vibration, vol. 286, no. 1-2, pp. 187-205, 2005.

- [5] Z. Jin-Yu, C. Yan, and H. Xiang-Xiang, “*Edge Detection of Images Based on Improved Sobel Operator and Gradient and Genetic Algorithms*,” in International conference on Image Analysis and Signal Processing. IASP 2009, pp. 31-35, 2009.
- [6] [Gonzalez & Woods, 2002] R. Gonzalez, and R. Woods, “*Digital Image Processing 2nd Edition*,” Prentice Hall, 2002.